Human Molecular Genetics, 2006, Vol. 15, No. 18 ***2791–2803***
doi:10.1093/hmg/ddl221
Advance Access published on August 29, 2006

Characterization of recessive RYR1 mutations in core myopathies

Haiyan Zhou[1,†], Naohiro Yamaguchi[2,†], Le Xu[2], Ying Wang[2], Caroline Sewry[3], Heinz Jungbluth[1,4], Francesco Zorzato[5], Enrico Bertini[6], Francesco Muntoni[1], Gerhard Meissner[2] and Susan Treves[7,*]

[1]The Dubowitz Neuromuscular Centre, Imperial College, Hammersmith Hospital, London W120NN, UK, [2]Department of Biochemistry and Biophysics, University of North Carolina, Chapel Hill, NC 27599-7260, USA, [3]Centre for Inherited Neuromuscular Disorders, Robert Jones and Agnes Hunt Orthopaedic Hospital NHS Trust, Oswestry SY10 7AG, UK, [4]Department of Paediatric Neurology, Evelina Children's Hospital, St Thomas' Hospital, London, UK, [5]Dipartimento di Medicina Sperimentale e Diagnostica, Universita'di Ferrara, 44100 Ferrara, Italy, [6]Unit of Molecular Medicine, Ospedale Bambin Gesu', Rome, Italy and [7]Departments of Anaesthesia and Research, Basel University Hospital, 4031 Basel, Switzerland

Received July 14, 2006; Revised and Accepted August 3, 2006

We have characterized at the molecular level, three families with core myopathies carrying apparent recessive mutations in their *RYR1* gene and studied the pharmacological properties of myotubes carrying endogenous mutations as well as the properties of mutant channels expressed in HEK293 cells. The proband of family 1 carried p.Ala1577Thr + p.Gly2060Cys in *trans*, having inherited a mutation from each parent. Immunoblot analysis of proteins from the patient's skeletal muscle revealed low levels of ryanodine receptor (RyR1) but neither substitution alone or in combination affected the functional properties of RyR1 channels in a discernable way. Two affected siblings in family 2 carried p.Arg109Trp + p.Met485Val substitutions in *cis*, inherited from the unaffected father. Interestingly, both affected siblings only transcribed the mutated paternal allele in skeletal muscle, whereas the maternal allele was silent. Single-channel measurements showed that recombinant, mutant RyR1 channels carrying both substitutions lost the ability to conduct Ca^{2+}. In this case as well, low levels of RyR1 were present in skeletal muscle extracts. The proband of family 3 carried p.Ser71Tyr + p.Asn2283His substitutions in trans. Recombinant channels with Asn2283His substitution showed an increased activity, whereas recombinant channels with p.Ser71Tyr + p.Asn2283His substitution lost activity upon isolation. Taken together, our data suggest major differences in the ways *RYR1* mutations may affect patients with core myopathies, by compromising RyR1 protein expression, stability and/or activity.

INTRODUCTION

The skeletal muscle ryanodine receptor (*RYR1*) gene encodes the sarcoplasmic reticulum junctional face membrane calcium release channel ryanodine receptor (RyR1), which plays a crucial role in excitation–contraction (E–C) coupling (1–6). The RyR1 ion channels are large protein complexes composed of four RyR 560 kDa peptides and various associated proteins with a total molecular weight of >2500 kDa. They play a crucial role in skeletal muscle E–C coupling by releasing calcium ions required for muscle contraction from the sarcoplasmic reticulum. Disease phenotypes associated with more than 80 dominant *RYR1* mutations identified to date include central core disease (CCD) (OMIM no. 117000) and the malignant hyperthermia susceptibility (MHS) trait (MH; OMIM no. 145600) (reviewed in 7–10). More recently, few

*To whom correspondence should be addressed at: Departments of Anesthesia and Research, Basel University Hospital, Hebelstrasse 20, 4031 Basel, Switzerland. Tel: +41 61 265 2373; Fax: +41 61 265 3702; Email: susan.treves@unibas.ch
†The authors wish it to be known that, in their opinion, the first two authors should be regarded as joint First Authors.

recessive mutations have been reported in association with patients affected by multi-minicore disease (MmD) (OMIM no. 602771) (11–14) and forms of CCD with unusual or more severe presentations (15). MHS-related *RYR1* mutations are predominantly located in the hydrophilic N-terminal and central portions of the RyR1 protein, whereas CCD-related *RYR1* substitutions mainly occur in the hydrophobic pore-forming region of the channel (16–21). To date, only few recessive *RYR1* mutations have been identified and they appear to be distributed throughout the entire gene (11,12,14) (Zhou *et al*., personal communication).

Investigation on the functional properties of *RYR1* mutations is crucial for the understanding of the molecular mechanisms associated with *RYR1*-related clinical phenotypes. Although it is widely accepted that MH-causing *RYR1* mutations increase the sensitivity of the RyR1 to activation by pharmacological reagents such as caffeine or 4-chloro-*m*-cresol (22–26) and CCD mutations attenuate channel activity and Ca^{2+} conductance (20,21,26–29), the molecular mechanisms associated with recessively inherited *RYR1*-related phenotypes are currently only partially understood (30).

In the following report, we identified *RYR1* mutations in three families with clinical features of a congenital myopathy with multiple cores on muscle biopsy. Functional properties of these *RYR1* mutants were distinct from those previously reported in CCD and depended on the substituted residues and their location: (i) the presence of the p.Ala1577Thr + p.Gly2060Cys substitutions in *trans* (in family 1) reduced RyR1 expression level, without noticeably affecting the functional properties of the recombinant RyR1 ion channel; (ii) the compound p.Arg109Trp + p.Met485Val substitutions in *cis* in family 2 also reduced the endogenous RyR1 expression level in muscle, but in addition affected the ability of recombinant channels expressing both substitutions to conduct Ca^{2+}; (iii) the p.Ser71Tyr and p.Asn2283His substitutions in *trans* in family 3 affected both channel stability and activity. These results suggest that some *RYR1* mutations may not only affect Ca^{2+} homeostasis directly, but also impair RyR1 function because they significantly affect the stability of the RyR1 complex. Finally, this report shows that in some patients harbouring *RYR1* mutations the disease phenotype is associated with silencing of the 'normal' allele.

RESULTS

Patient phenotype, mutation screening, histological examination and family history

In this study, we examined four patients from three different families displaying a similar clinical phenotype: all patients presented clinical manifestations during the neonatal period showing muscle weakness, hypotonia and feeding difficulties, followed by delayed motor milestones. One of the two siblings in family 2 required prolonged ventilation in the neonatal period; the affected child in family 3 had bilateral hip dysplasia for which he was operated at the age of 3 months; the propositus in family 1 had bilateral talipes for which surgery was performed at the age of 10 months. Marked axial weakness and feeding difficulties with subsequent poor weight gain characterized all affected children, requiring gastostomy intervention in the two siblings of family 2 who also had ophthalmoplegia. All affected children acquired the ability to walk, although late, between 18 and 24 months, and they remain ambulant but only for relatively short distance. They all have difficulties in rising from the floor and climbing stairs; respiratory muscle weakness leading to frequent chest infection was a particularly prominent feature in families 1 and 2 and indicates a more severe phenotype of these families compared with family 3.

Figure 1 shows the family tree and genetic characterization of the patients and their family members studied. The three families carried compound heterozygous substitutions in their *RYR1*. Screening of the entire *RYR1* cDNA was performed in order to exclude the presence of other amino acid substitutions.

In family 1, the p.Ala1577Thr substitution was transmitted from the mother and was not found in 100 control chromosomes, whereas the paternally transmitted p.Gly2060Cys substitution was previously reported as a polymorphism (7,31). We determined the frequency of the polymorphic p.Gly2060Cys substitution in 50 individuals of the general population and 28 patients affected by core myopathies. Seven controls and four patients carried this variation, indicating a similar distribution in the two populations, further suggesting this to be a polymorphism.

The two siblings in family 2 showed transcription of only one allele in muscle, whereas they clearly carried two alleles at the genomic level. These patients transcribed in muscle the allele containing the two substitutions p.Arg109Trp and p.Met485Val, inherited from the asymptomatic father. However, p.Met485 is not a conserved residue and shows as leucine in all other species, suggesting it probably as a polymorphism.

In family 3, the patient harbours two substitutions, p.Ser71Tyr and p.Asn2283His transmitted each from one asymptomatic parent. The monozygotic twins are apparently asymptomatic but could not be studied genetically.

The presence of the mutations was confirmed by RT–PCR analysis using myotubes derived from satellite cells in family 1 and using myotubes derived from skin fibroblasts transduced with MyoD-encoding adenovirus in families 2 and 3 (discussed subsequently). Figure 1C shows the results obtained after PCR amplification and sequencing. In the proband of family 3, the cDNA from MyoD-transformed myotubes has a genotype identical to that found in the patient's muscle tissue. Interestingly, in family 2, both the paternal and maternal alleles were transcribed in the fibroblasts transduced with MyoD. This clearly differed from the pattern of transcription in the skeletal muscle biopsies, in which only the paternal allele was transcribed (described earlier).

The histopathological features of the biopsies from the three affected families are compatible with those now known to be associated with *RYR1* mutations. The muscle biopsy from patient 1 showed mild variation in fibre size, an increase in internal nuclei, some of which were central, and a little endomysial connective tissue (Fig. 2A). Oxidative enzyme staining revealed multiple focal areas devoid of stain, as well as some single cores of moderate size, and some peripheral aggregation of stain (Fig. 2D and G). Fibre typing was indistinct with NADH-TR staining and most fibres expressed slow myosin.

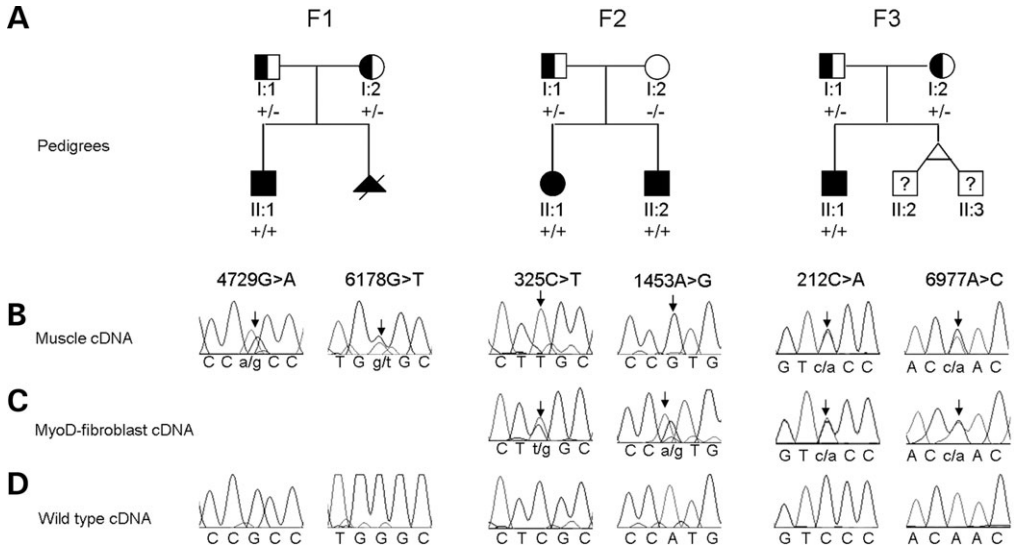

Figure 1. Pedigrees and genotyping data of the three families with mini-core myopathy investigated in the present study. (**A**) Pedigrees of the three families carrying compound heterozygous mutations in their *RYR1* gene. Black symbols: symptomatic core myopathy patients; open symbols: asymptomatic individuals; half-black symbols: carriers; triangle symbol with line through: affected, termination of pregnancy; question marks: untested individuals. Plus indicates the presence of the mutated allele and minus indicates the presence of the normal allele. (**B**) Chromatograms obtained from sequencing muscle tissue RyR1 cDNA. Arrows indicate the residues giving rise to nucleotides variations. At variance from the heterozygous variations identified in F1 and F3, the nucleotide variations found in F2 show homozygous changes. (**C**) Chromatograms obtained from sequencing the RyR1 cDNA from myotubes obtained after myoD transduction of skin fibroblasts. In F2, the nucleotide variations present as heterozygous changes were present both at the genomic level (data not shown) and at the transcriptional level in myotubes derived from myoD-transduced fibroblasts, but as homozygous changes in muscle tissue. In F3, the genotypes of the cDNAs derived from muscle and from myotubes derived from myoD-transduced fibroblasts are the same. (**D**) Chromatograms for the sequencing of WT muscle cDNA.

The biopsy from one affected child in family 2 showed a wide variation in fibre size with atrophy and hypertrophy. Several fibres had internal nuclei, many of which were central (Fig. 2B). Some fibres also showed red stained rod-like structures with the Gomori trichrome stain. Oxidative enzyme stains showed large areas devoid of stain, and obliquely sectioned fibres suggested that these core areas were focal but often spanned the width of the fibre (Fig. 2E and H). Fibres with slow myosin were predominant.

The muscle biopsy from the affected child in family 3 showed moderate variation in fibre size and no increase in internal nuclei (Fig. 2C). Oxidative enzyme stains showed prominent core areas in several fibres, which were often peripheral, as well as unevenness of oxidative enzyme stain and uniform fibre typing (Fig. 2F). No longitudinally sectioned fibres were present from this biopsy to assess the length of the cores.

Immunoblot analysis of muscle samples

Western blot analysis on total protein extracts revealed low levels of RyR1 in the total protein extract from the muscle from patients of families 1 and 2 harbouring the p.Ala1577Thr + p.Gly2060Cys (Fig. 3, lane 1) and p.Arg 109Trp + p.Met485Val (Fig. 3, lane 2) substitutions compared with the control. Muscle samples from the p.Ser71Tyr + p.Asn2283His patient and control showed similar levels of RyR1 (Fig. 3, lanes 3 and 4); the intensity of the immunoreactive band corresponding to desmin was similar in all samples tested. The results suggest that the RyR1 mutations in families 1 and 2 affect RyR1 protein expression and/or stability.

MyoD-transduced fibroblasts express proteins characteristic of differentiated skeletal muscle

We also considered the possibility that the amino acid substitutions may compromise RyR1 function by performing cellular Ca^{2+} release measurements in myotubes. Because myotubes derived from satellite cells of muscle biopsies are not always available, and in our case were not available from families 2 and 3, in initial experiments we tested whether myotubes obtained by adenovirus-mediated MyoD transduction of control skin fibroblasts could be used to characterize the RyR1 mutants. Figure 4 shows indirect immunofluorescence analyses of untransduced fibroblasts (left panels) or skin fibroblasts from a control, transduced with MyoD and differentiated for 5–7 days (right panels). We found that the differentiated cells express markers of skeletal muscle cells such as desmin and myosin; they also express both the dihydropyridine receptor (DHPR) and the RyR1. No immunoreactivity was present for these skeletal muscle proteins in skin fibroblasts. Figure 5A shows that myotubes derived from MyoD-transduced fibroblasts also express a functional RyR1 ion channel, as stored Ca^{2+} could be released via the DHPR, by adding 150 mM KCl (Fig. 5A) and pharmacologically by 4-chloro-*m*-cresol (which activates RyR1 independent of DHPR) (Fig. 5B). Figure 5C compares the sensitivities to pharmacological activation of control myotubes derived from differentiating myoblasts by serum deprivation with those derived from control MyoD-transduced fibroblasts. The peak of the Ca^{2+} transients elicited by agonist was determined and used to construct dose-dependence curves. Both kinds of myotubes respond to KCl, 4-chloro-*m*-cresol and caffeine: the maximal increase in fluorescence and EC_{50} for

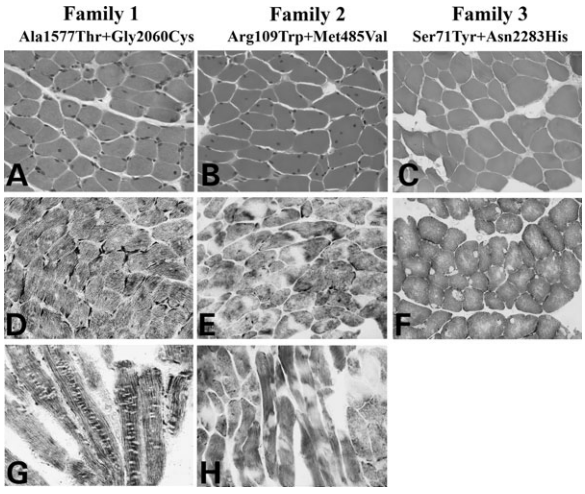

Figure 2. Histolopathological features of muscle biopsies from patients with core myopathy. Haematoxylin and eosin (**A**–**C**), NADH-TR (**D** and **G**) and cytochrome oxidase (**E**, **F** and **H**). Note the increase in internal nuclei in families 1 and 2 (A and B), and that fibre typing is indistinct all three cases. In family 1, multiple cores are clearly seen (D and G); in family 2, the prominent cores often span the width of the fibre (E and H) and in family 3, the large cores are often peripheral and there is also uneven staining (F).

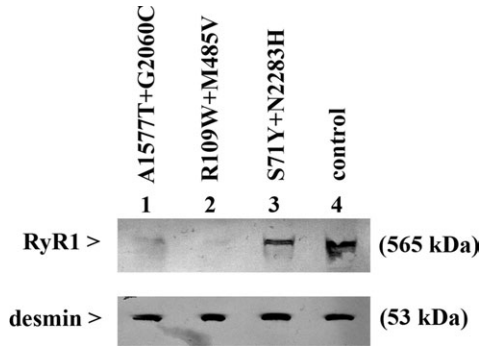

Figure 3. Western blot of total protein extracts from skeletal muscle biopsies of patients with *RYR1* mutations. Lane 1: p.Ala1577Thr + p.Gly2060Cys, lane 2: p.Arg109Trp + p.Met485Val, lane 3: p.Ser71Tyr + p.Asn2283His, lane 4: control. Thirty micrograms of proteins were loaded on a 3–8% NuPAGE pre-cast gel and transferred electrophoretically to nitrocellulose membrane; the blot was probed with anti-RyR1 and anti-desmin antibodies as described in Materials and Methods. Desmin immunoreactivity was used as muscle-specific internal control.

KCl and caffeine was not significantly different (F_{max} and EC_{50} for KCl were 0.22 ± 0.04 and 35.4 ± 6.5 versus 0.25 ± 0.03 and 30.7 ± 3.0, and for caffeine, they were 0.29 ± 0.028 and 6.3 ± 0.54 versus 0.36 ± 0.03 and 8.07 ± 0.72 in control and MyoD myotubes, respectively). Control and MyoD myotubes showed also similar peak Ca^{2+} transient in the presence of 600 μM 4-chloro-*m*-cresol (0.28 ± 0.04 versus 0.29 ± 0.03, respectively). However, at higher agonist concentrations, the curve did not saturate in MyoD myotubes, indicating that non-specific Ca^{2+} release due to activation of other intracellular receptors/channels might be occurring. These results confirm the validity of the MyoD myotube model assessing the effects of RyR1 mutations on stored Ca^{2+} release, when satellite-cell-derived myotubes from patients are not readily available.

Effect of RyR1 amino acid substitutions on resting cytosolic Ca^{2+} concentrations and stored Ca^{2+} release

We used the fluorescent Ca^{2+} indicator Fura-2 to determine whether the *RYR1* mutations identified in the core myopathy patients affected resting cytosolic Ca^{2+} concentrations ($[Ca^{2+}]_i$) of myoD-tranduced myotubes obtained from (i) compound heterozygous affected individuals, (ii) heterozygous parents when available and (iii) control individuals (Fig. 6). The resting fluorescence ratio observed in cells from affected patients and healthy parents was not significantly different from that observed in control cells, for all amino acid substitutions, except for cells carrying the p.Ser71Tyr + p.Asn2283His *RYR1* substitution ($P < 0.00001$) (Fig. 6). Of interest, the resting $[Ca^{2+}]_i$ of myotubes derived from MyoD-transduced fibroblasts was slightly lower (10–20 nM) than that observed in myotubes derived from primary muscle cultures.

Next we determined whether a decrease in SR Ca^{2+} release was responsible for the weak muscle phenotype of the patients harbouring recessive *RYR1* mutations. Table 1 compares the peak Ca^{2+} release (R_{max}) obtained by treating myotubes with KCl and caffeine. None of the substitutions caused a significant decrease in the peak Ca^{2+} release when compared with that observed from control cells or cells obtained from unaffected family members. Of interest, cells carrying the p.Ser71Tyr + p.Asn2283His *RYR1* substitution were more sensitive to RyR1 activation and behaved like cells from MHS individuals. Although peak Ca^{2+} release (R_{max}) was not significantly affected (Table 1), the EC_{50} was reduced by ~50% (from 20.1 ± 0.03 to 10.7 ± 0.04 for KCl and 6.1 ± 1.2 to 1.9 ± 0.1 for caffeine in MyoD myotubes from control and p.Ser71Tyr + p.Asn2283His, respectively).

Functional properties of mutant RYR1s expressed in HEK293 cells

In order to gain a more comprehensive view of the effects of the mutations on RyR1 channel function, we expressed rabbit RyR1s carrying the recessive mutations in a heterologous (HEK293) cell system that lacks endogenous RyRs. Note that in the cells expressing the recombinant rabbit RyR1 cDNA, the rabbit nomenclature for residues is used. The expression levels and functional properties of the recombinant RyR1 mutants were determined by cellular fluorescence microscopy, immunoblot analysis and [^{3}H]ryanodine binding. Single channels were recorded to determine the ion permeation properties of the mutants.

The fluorescence change of Fluo-4 was measured to detect Ca^{2+} release in response to 10 mM caffeine or 400 μM 4-chloro-*m*-cresol in HEK293 cells that expressed wild-type (WT) and mutant RyR1s. Similar time courses and peak amplitudes of Ca^{2+} release were observed for cells expressing WT and Ala1578Thr, Ser2060Cys, Leu486Val, Ser71Tyr and Asn2283His *RYR1* mutant channels, whereas vector-transfected cells and cells transfected with cDNAs carrying Arg110Trp or Arg110Trp + Leu486Val substitutions showed

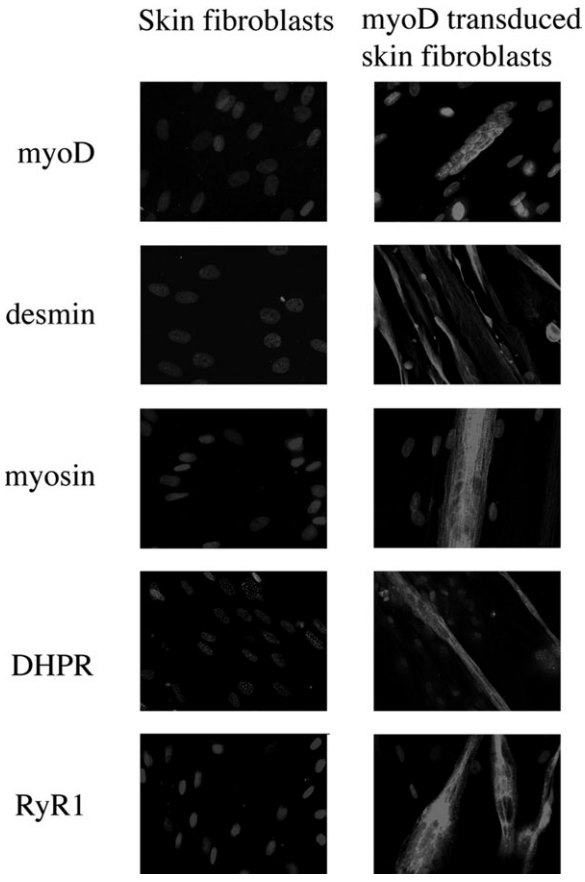

Figure 4. Photomicrograph of cultured skin fibroblasts before and after MyoD transduction and differentiation into myobasts. *Left*: fibroblasts established from skin biopsies and cultured as described in Materials and Methods. *Right*: myotubes derived from MyoD transduction and cultured in differentiation medium for 5–8 days. Panels show photomicrographs of cells after indirect immunofluorescence staining for MyoD, desmin, myosin, α1.1 subunit of the DHPR and skeletal muscle RyR1. (20 × 0.5 HC PL FLUOTAR objective).

no caffeine and 4-chloro-*m*-cresol response (data not shown). Immunoblot analysis showed that the absence of caffeine and 4-chloro-*m*-cresol responses was not due to lack of protein expression as both the single and double RyR1 mutants were expressed in HEK293 cells at a level comparable to WT (data not shown).

The expression of functional RyR1 mutants was also assessed by a [^{3}H]ryanodine binding assay. Ryanodine binds with high specificity to the RyRs and is widely used as a probe of channel activity because of its preferential binding to the open channel state (32). Membrane fractions isolated from HEK293 cells expressing the Ala1578Thr, Ser2060Cys, Leu486Val and Asn2283His *RYR1* mutants bound [^{3}H]ryanodine (Fig. 7A) and showed Ca^{2+} dependence of [^{3}H]ryanodine binding (Fig. 7B) close to those of WT-RyR1. Figure 7C shows that caffeine increased [^{3}H]ryanodine binding to microsomes harbouring WT RyR1 and RyR1s carrying the Ala1578Thr, Ser2060Cys, Leu486Val and Asn2283His substitutions. Interestingly, Asn2283His recombinant channels bound an increased amount of [^{3}H]ryanodine (normalized to B_{max} value) in the absence of caffeine, however, without showing an increased caffeine sensitivity. Two RyR1 mutants (Arg110Trp and Arg110Trp + Leu486Val) showed loss of high-affinity [^{3}H]ryanodine binding (Fig. 7A), in agreement with our observation that these two mutants failed to show a caffeine or 4-chloro-*m*-cresol response in HEK293 cells. RyR1-Ser71Tyr exhibited a caffeine and 4-chloro-*m*-cresol response in HEK293 cells but failed to bind substantial amounts of [^{3}H]ryanodine, which indicated a loss of function during membrane isolation.

We also expressed in HEK293 cells RyR1-Ala1578Thr and RyR1-Ser2060Cys or RyR1-Ser71Tyr and RyR1-Asn2283His mutants in 1:1 ratio to match their simultaneous expression in families 1 and 3. Co-expression of RyR1-Ala1578Thr and RyR1-Ser2060Cys yielded a B_{max} value (Fig. 7A) and Ca^{2+}-dependence (Fig. 7B) of [^{3}H]ryanodine binding comparable to those for membranes isolated from cells carrying the two mutants alone. Co-expression of RyR1-Ser71Tyr and RyR1-Asn2283His also showed the presence of functional RyR1 channels, albeit at a reduced level, as these cells exhibited a B_{max} value of [^{3}H]ryanodine binding intermediate to cells expressing the two mutants alone.

Figure 8 compares single-channel activities and ion permeation properties of WT ion channels with two mutant channels. Shown are RyR1-Asn2283His which exhibited an apparent increased activity in [^{3}H]ryanodine binding experiments and RyR1-Arg110Trp + Leu486Val which failed to show a caffeine and 4-chloro-*m*-cresol response in HEK293 cells. Single-channel measurements were performed using the planar lipid bilayer method. Proteoliposomes containing the purified channels were fused with planar lipid bilayers, and single channels were initially recorded in 250 mM KCl on both sides of the bilayer with K^+ as the current carrier. The cis (cytosolic) and trans (SR lumenal) bilayer chambers contained micromolar-activating Ca^{2+} (2 μM). To ascertain retention of pharmacological regulation, cytosolic Ca^{2+} concentrations were reduced to 0.1 μM. To determine Ca^{2+} currents (at 0 mV) as well as Ca^{2+} selectivity, WT and mutant channels were recorded in 250 mM symmetrical KCl with 10 mM Ca^{2+} in the trans (SR lumenal) bilayer chamber. We found that RyR1-Asn2283His showed an increased single-channel open probability (P_o) compared with WT at both 2 and 0.1 μM cis Ca^{2+} as well as with 10 mM trans Ca^{2+} as conducting ion (Fig. 8A and B, Table 2). Kinetic analysis showed that the mutation increased P_o at 2 μM cytosolic Ca^{2+} by raising the mean open time without significantly changing the number of single-channel events or mean close time (legend of Fig. 8). Single-channel activities of RyR1-Arg110Trp + Leu486Val were high, but did not respond to a change in cytosolic Ca^{2+} concentration (Fig. 8A, Table 2). Moreover, no single-channel currents were measured at 0 mV with 10 mM Ca^{2+} in the trans chamber.

K^+ currents of WT, Arg110Trp + Leu486Val and Asn2283His RyR1 channels, measured in symmetrical 250 mM KCl, showed a linear voltage-dependence (Fig. 8C). Single-channel conductances were not different for WT and RyR-Asn2283His but were highly variable for RyR Asn2283His, yielding an averaged reduced K^+ conductance of 442 ± 77 pS (Table 2). In the presence of 10 mM Ca^{2+} trans at 0 mV, Asn2283His exhibited a unitary Ca^{2+} current essentially identical to that of WT RyR1 (Fig. 8C, Table 2).

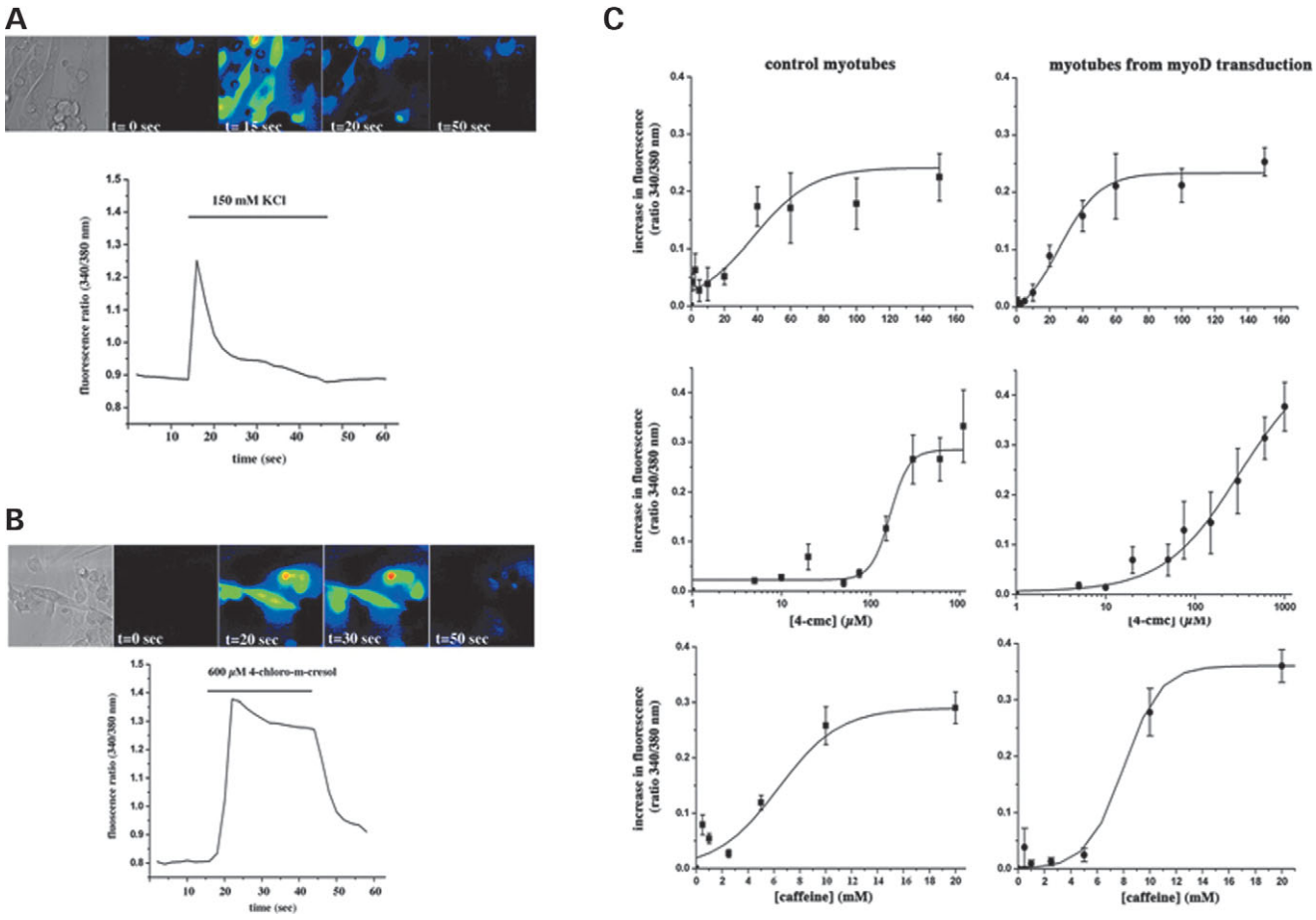

Figure 5. Calcium release stimulated by KCl and 4-chloro-*m*-cresol in myotubes derived from myoD-transduced fibroblasts established from control individuals. Single cell intracellular Ca^{2+} measurements of fura-2 loaded cells in response to 150 mM KCl (**A**) and 600 μM 4-chloro-*m*-cresol (**B**). *Top* (from left): phase contrast; resting $[Ca^{2+}]_i$ before the application of 150 mM KCl; 15, 20 and 50 s after the application of the indicated agonist. Myotubes were individually stimulated by addition of the agonist in Krebs–Ringer buffer containing no added Ca^{2+} and 100 μM La^{3+}, thus the increase in $[Ca^{2+}]_i$ represents only release of calcium from intracellular stores. Plotted trace represents change in $[Ca^{2+}]_i$ (fluorescence ratio 340/380 nm) of a single cell. (**C**) Comparison of calcium release after pharmacological RyR1 activation myotubes and myotubes derived from myoD-transduced fibroblasts. Curves show the KCl, 4-chloro-*m*-cresol and caffeine dose-dependent changes in calcium, expressed as Δ in fluorescence ratio (peak ratio 340/380 nm − resting ratio 340/380 nm). Each point represents the mean (±SE) of the Δ fluorescence of measurements performed on five to 20 different cells. Dose–response curves were generated using the Origin software.

Single-channel currents were reduced at elevated positive and negative potentials, and the reversal potentials (E_{rev}) for WT RyR1 and RyR-Asn2283His were shifted by +9.5 and +12.6 mV, respectively. Applying constant field theory, a permeability ratio of Ca^{2+} over K^+ (P_{Ca}/P_K) of 7.0 and 10.6 was calculated for WT and Asn2283His RyR1 channels, respectively (Table 2). In contrast, addition of 10 mM trans Ca^{2+} did not generate a noticeable unitary Ca^{2+} current at 0 mV and was without effect on K^+ currents or reversal potential of RyR1 Arg110Trp + Leu486Val (Fig. 8C, Table 2). Taken together, the single-channel data indicate that the Asn2283His mutation increases Ca^{2+} responsiveness and ion selectivity for Ca^{2+} compared with K^+, without altering K^+ conductance. In contrast, the homozygous Arg110Trp + Leu486Val mutations abolished Ca^{2+} responsiveness and Ca^{2+} permeation, and reduced the K^+ conductance, demonstrating that the homozygous expression of the Arg110Trp + Leu486Val mutations introduces major alterations to the channel pore.

DISCUSSION

In this report, we present data relative to newly identified RyR1 amino acid substitutions found in patients with core myopathies, from three families. Our results show that different mutations are associated with different functional outcomes: (i) the p.Ala1577Thr + p.Gly2060Cys and p.Arg109Trp + p.Met485Val mutations lead to a decrease in the amount of RyR1 expressed in skeletal muscle. (ii) Heterozygosity for p.Ser71Tyr + p.Asn2283His results in an 'unstable' protein that looses activity when isolated from HEK293 cells and conveys an MHS phenotype. The mutation responsible for the increased RyR1 sensitivity is the p.Asn2283His. (iii) The homozygous expression of p.Arg109Trp + p.Met485Val also affects Ca^{2+} transport and [^{3}H]ryanodine binding, leading to Ca^{2+} dysregulation. In family 2, both affected children exclusively transcribed in muscle the paternal allele carrying the two substitutions, despite being heterozygous at the genomic DNA level.

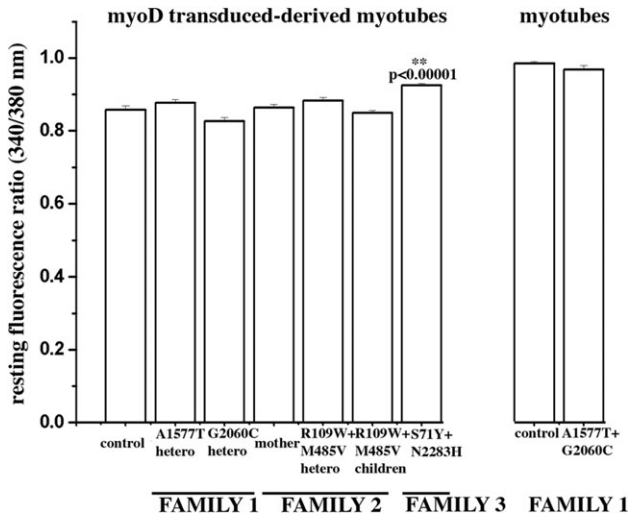

Figure 6. Resting calcium concentration of human myotubes from control individuals and individuals bearing the indicated *RYR1* substitutions. *Histograms on the left*: average resting myoplasmic [Ca^{2+}] of cells from controls, healthy parents and affected family members bearing the indicated *RYR1* substitutions. Measurements were made on myotubes derived from myoD-transduced fibroblasts 6 days after differentiation. *Histograms on the right*: average resting myoplasmic [Ca^{2+}] of myotubes from controls and from patient harbouring the compound heterozygous p.Ala1577Thr + p.Gly2060Cys substitutions. Measurements were made on cells established from muscle biopsies and differentiated into myotubes for 7–10 days. Values are the mean (±SE, $n = 41–157$) analysed cells. The $[Ca^{2+}]_i$ was measured using the fluorescent Ca^{2+} indicator fura-2, in Krebs–Ringer containing 1 mM $CaCl_2$ and 100 μM La^{3+}. The resting $[Ca^{2+}]_i$ was significantly higher only in cells harbouring the compound p.Ser71Tyr + Asn2283His compared with controls ($P < 0.00001$).

Thus, in addition to more 'conventional' effects of mutations, in some patients affected by core myopathies, haploinsufficiency or allele silencing must be verified, as the genotype of the genomic DNA may not always reflect the transcribed mRNA (Zhou *et al*., 2006, submitted for publication).

The presence of cores or areas devoid of oxidative enzyme activity and mitochondria exhibiting variable degrees of myofibrillar disruption, is a non-specific feature occurring in several neuromuscular disorders but appears to be a particular feature associated with mutations in the *RYR1* gene (33,34). In CCD, the large centrally located cores affecting an appreciable number of sarcomeres are predominantly caused by dominant mutations in the *RYR1* gene and cause dysregulation of myoplasmic Ca^{2+} homeostasis by affecting the amount of Ca^{2+} released after RyR1 activation (7,9,10). In other cases, the presence of multiple small cores, with several focal areas per fibre affecting only a few sarcomeres have been associated with recessive mutations in the *RYR1* gene; for one of these (the p.Pro3527Ser substitutions), we were able to show that its presence at the homozygous state also affects the amount of Ca^{2+} released after direct pharmacological activation of the RyR1 (30). Though some clinical features of patients with minicore myopathy may appear to overlap with those observed in patients with CCD, the two conditions can be distinguished, so it is not surprising that the functional effects of the underlying genetic defects are dissimilar. Of the three compound heterozygous mutations we investigated in this study, we found that the p.Ala1577Thr + p.Gly2060Cys did not affect Ca^{2+} homeostasis in any discernable way, i.e. the resting [Ca^{2+}], the pharmacological activation of Ca^{2+} release, the RyR1-dependent IL-6 release (data not shown) and the single-channel properties of recombinant channels harbouring these mutations were unaffected. Thus, either these substitutions are unrelated to the core myopathy and search for mutation(s) in other genes must be undertaken or the effect of the two substitutions operates by a distinct mechanism, for example, the mutations may interfere with the stability of the RyR1 macromolecular complex within the skeletal muscle. In line with this hypothesis, we found that the relative amount of RyR1 protein present in the muscle biopsy from the patient was significantly decreased, whereas the overall level of RyR1 transcript in the patient's muscle and the amount of RyR1 protein over-expressed in HEK293 cells transfected with the cDNA carrying these substitutions were not affected. Thus, the concomitant presence of both substitutions leads to a decrease in the stability of the RyR1 complex causing partial depletion of RyR1 Ca^{2+} channels in the skeletal muscle tissue of the patients. A similar finding was reported by Monnier *et al*. (35) in a patient with MmD and ophthalmoplegia carrying a homozygous splicing *RYR1* mutation; in their patient, the presence of a cryptic splicing mutation resulted in a 90% decrease in the normal RYR1 transcript in skeletal muscle.

As to family 2, western blot analysis revealed that the p.Arg109Trp + p.Met485Val substitutions were also accompanied by a reduction in the amount of RyR1 expressed in muscle tissue. Intracellular Ca^{2+} measurements on myotubes derived from MyoD-transduced fibroblasts showed little or no functional effects of the mutations at the heterozygous state. However, transcription analysis disclosed a fundamental difference between skeletal muscle and MyoD-transduced myoblasts, as the former tissue was monoallelic, whereas the latter showed biallelic transcription. It is therefore not surprising that the Ca^{2+} measurement in the MyoD-transduced myotubes did not reveal alterations in Ca^{2+} homeostasis. Importantly, when HEK293 cells carrying

Table 1. Ability of cells carrying the indicated *RYR1* mutations to release calcium after pharmacological RyR1stimulation

	Patient	KCl R_{max}	Caff R_{max}
	MyoD myotubes control	0.25 ± 0.03	0.36 ± 0.03
	Myotubes from control	0.22 ± 0.04	0.29 ± 0.03
Family 1	A1577T heterozygous	0.27 ± 0.04	0.33 ± 0.04
	G2060C heterozygous	0.29 ± 0.07	0.21 ± 0.06
	A1577T + G2060C compound heterozygous	0.32 ± 0.04	0.31 ± 0.09
Family 2	Control mother	0.28 ± 0.04	0.25 ± 0.06
	R109W + M485V heterozygous father	0.21 ± 0.04	0.10 ± 0.07
	R109W + M485V+ heterozygous children[a]	0.21 ± 0.01	0.11 ± 0.02
Family 3	S71Y+ N2283H compound heterozygous	0.24 ± 0.04	0.17 ± 0.03

[a]MyoD-transduced fibroblasts from these patients carried the same genotype as the unaffected father and were heterozygous for both substitutions, whereas muscle from the patients only expressed the mutated allele.

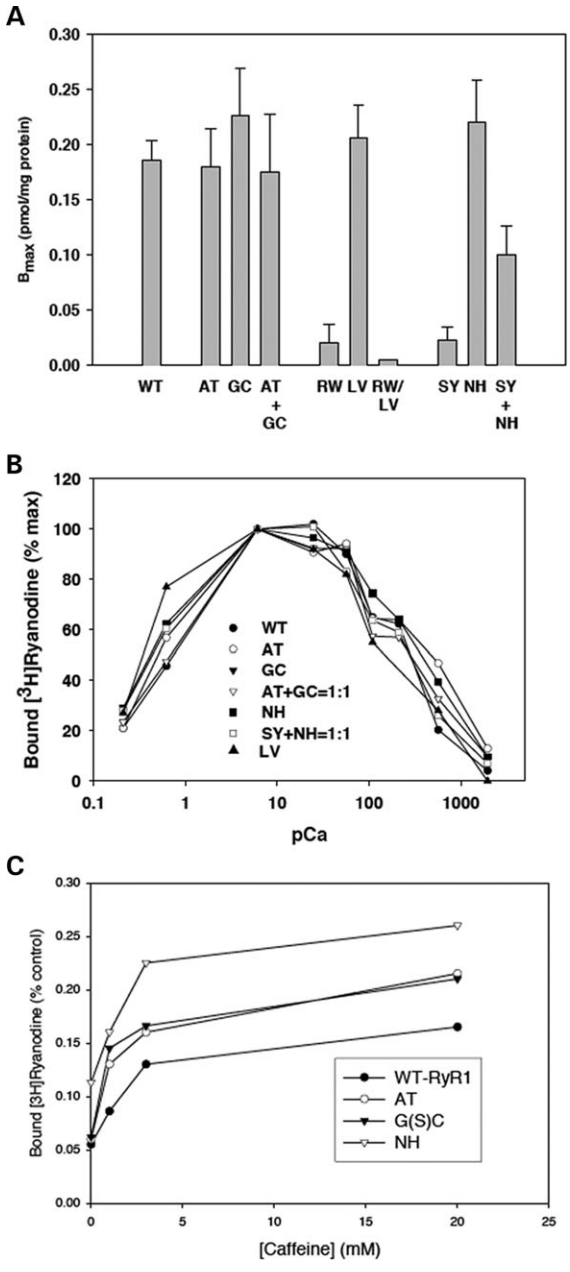

Figure 7. Functional properties of WT and mutant RyR1 channels. (**A**) B_{max} values of [^{3}H]ryanodine binding to WT-RyR1, RyR1 single-site mutants Ala1578Thr (AT), Ser2060Cys (GC), Arg110Trp (RW), Leu486Val (LV), Ser71Tyr (SY) and Asn2283His (NH), RyR1 double mutant RW/LV and single-site mutants AT + GC and SY + NH transfected in 1:1 ratio. Data are the mean ± SE of three to 12 experiments. (**B**) Ca^{2+} dependence of [^{3}H]ryanodine binding to WT-RyR1 and RyR1 mutants. Specific [^{3}H]ryanodine binding for cells transfected with WT-RyR1 and RyR1 mutants was determined in 250 mM KCl, 150 mM sucrose, 20 mM imidazole, pH 7.0, and 1 mM glutathione (oxidized) media containing 3 nM [^{3}H]ryanodine and the indicated concentrations of free Ca^{2+}. Data are mean of three to seven experiments. SE were less than 20%. (**C**). Caffeine dependence of [^{3}H]ryanodine binding to WT and mutant RyR1s. Specific [^{3}H]ryanodine binding to WT-RyR1 (closed circles) and RyR1 mutants Ala1578Thr (open circles), Ala1578T + Ser2060Cys (open triangles), Ser71Tyr (open squares), Leu486Val (closed triangles) and Asn2283His (closed squares) was determined in 0.25 M KCl, 20 mM imidazole, pH 7 solution containing 0.5 μM free Ca^{2+}, 4 nM [^{3}H]ryanodine and indicated concentrations of caffeine. Data are the mean ± SE of three to 12 experiments.

recombinant homozygous channels were analysed, the results were different: channels bearing the two substitutions inherited from the father were unable to transport Ca^{2+} and did not bind [^{3}H]ryanodine. Of the two substitutions that were co-expressed, the p.Arg109Trp alone was sufficient to significantly diminish [^{3}H]ryanodine binding to recombinant RyR1. Therefore, in this family, two mechanisms may partake in causing the myopathy: Ca^{2+} dysregulation due to the homozygous expression of the pArg109Trp residue in the patient's skeletal muscle and the concomitant instability of the RyR1 carrying both homozygous substitutions leading to a reduction in the levels of RyR1 protein within skeletal muscle. In this context, it should be mentioned that the clinical phenotypes of patients from both families 1 and 2, in whom we found partial depletion of endogenous RyR1 Ca^{2+} channels, were more severe compared with the patient from family 3.

As far as the p.Ser71Tyr + p.Asn2283His substitutions found in family 3 are concerned, our results demonstrate that their presence leads to unstable channels because no [^{3}H]ryanodine binding was observed on microsomes from transfected HEK293 cells even though control levels of RyR1 were detected on western blots from transfected HEK293 cells and in muscle biopsies. Thus, though in family 3 the mutations do not lead to a significant reduction in RyR1 protein content, we can hypothesize that they affect the stability of the RyR1 macromolecular complex. An additional observation emerging from this study is that myotubes carrying the p.Ser71Tyr + p.Asn2283His substitutions had a significantly higher resting [Ca^{2+}] and a shift in the sensitivity to pharmacological RyR1 activation, typical features of MHS (24,26,36), and our results support that p.Asn2283His substitution is responsible for conveying the MHS phenotype.

This study also explored the possibility of using primary cultures of fibroblast to study the defects of the protein machinery involved in skeletal muscle E–C coupling, when primary muscle cell cultures are not available. This system offers obvious advantages including the ease of obtaining skin patch biopsies even from children, the capacity of fibroblasts to proliferate rapidly in culture and to be induced to differentiate into myotubes after transduction with MyoD. Nevertheless, our study also has identified some limitations associated with the use of such cells as (i) the cell's genotype should be carefully evaluated in order to confirm that it matches that of the patient's muscle, in order to exclude silencing for the mutation(s) under investigation. (ii) Their resting [Ca^{2+}] is slightly, but significantly lower than that found in myotubes derived from primary muscle cultures and their response to 4-chloro-*m*-cresol does not saturate. The latter observation may be due to the fact that such cells may also express type 3 RyR which may be activated at millimolar concentrations of 4-chloro-*m*-cresol (37,38). As to higher resting [Ca^{2+}] of myotubes derived from primary muscle cell cultures, this probably reflects the pathways which are undertaken during myoblast differentiation: during 'physiological' myogenesis, the expression of Kir2.1 channels on the plasma membrane cause myoblast hyperpolarization, activation of myogenin and MEF-2 transcription factors and the appearance of T-type Ca^{2+} channels which increase the myoplasmic Ca^{2+} concentration by allowing an influx of Ca^{2+} through the plasma membrane (39,40). In contrast, transduction with MyoD artificially induces fibroblasts to initiate a myogenic

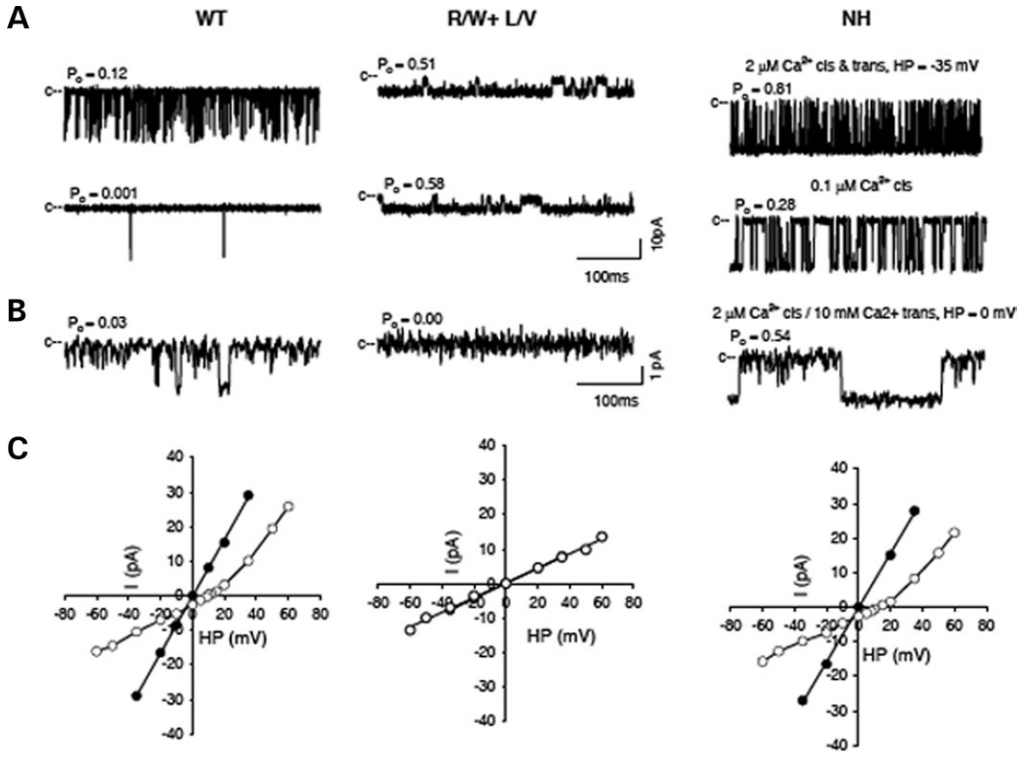

Figure 8. Single-channel activities of WT, Arg110Trp + Leu486Val and Asn2283His RyR1 ion channels. (**A**) Traces represent single-channel currents (openings shown as downward deflections from the closed state, c) of WT RyR1 (left), Arg110Trp + Leu486Val (middle) and Asn2283His (right) at −35 mV recorded in symmetrical 250 mM KCl and indicated concentrations of free cis (cytosolic) Ca^{2+}. Averaged single-channel parameters at 2 μM Ca^{2+} cis were for WT-RyR1 and Asn2283His, respectively, $P_o = 0.24 \pm 0.04$ (16) and $0.55 \pm 0.07^*$ (10), events/min = 19248 ± 2349 and 16509 ± 1586, $T_o = 0.66 \pm 0.06$ and 2.11 ± 0.50 ms*, $T_c = 4.82 \pm 1.99$ and 1.46 ± 0.21 ms. Channel parameters were calculated from recordings that contained a single-channel activity. $^*P < 0.05$ compared with WT. (**B**) Traces represent single-channel currents of WT, Arg110Trp + Leu486Val and Asn2283His at 0 mV in symmetrical 250 mM KCl in the presence of 10 mM trans (SR lumenal) Ca^{2+} and 2 μM free Ca^{2+} cis. (**C**) Current voltage relationships of WT, Arg110Trp + Leu486Val and Asn2283His RyR1 channels in symmetrical 250 mM KCl (filled circles) and following addition of 10 mM trans Ca^{2+} (open circles).

differentiation without the coordinated and stepwise activation of physiological transcription factors.

In conclusion, we have identified novel *RYR1* substitutions in patients with core myopathies and demonstrate that the functional impact of the mutations is complex and different from those typically observed in patients with CCD carrying dominant *RYR1* mutations. These substitutions lead to a decrease in RyR1 content within the muscle and/or a decrease in the stability of isolated channels; in one case, the mutations at the homozygous state were also accompanied by the inability to transport Ca^{2+}. These results indicate the importance of assessing not only the functional properties of mutated RyR1 channels in core myopathy patients, but also, when possible, the transcriptional status and endogenous muscle RyR1 levels in patients.

MATERIALS AND METHODS

Materials

Fura-2/AM was from Calbiochem. Caffeine was from Merck (Darmstadt, Germany), 4-chloro-*m*-cresol was from Fluka Chemicals (Buchs, Swizerland). Mouse anti-MyoD monoclonal antibody was from BD Biosciences (Belgium), mouse anti-desmin monoclonal antibody was from DAKO (Denmark), mouse anti-slow muscle myosin monoclonal antibody was from Chemicon (CA, USA), goat anti-DHPR polyclonal antibody was from Santa Cruz (USA) and mouse anti-RyR1 monoclonal antibody was from Abcam (Cambridge, UK). The secondary biotinylated anti-mouse Ig antibody, Hybond-ECL nitrocellulose and ECL plus Chemiluminescence kit were from Amersham (Buckinghamshire, UK). Streptavidine conjugated to Alexa Fluor-594 and Hoechst 33342 were from Molecular Probes (Leiden, The Netherlands). RNA isolation system was from Qiagen. The SuperScript™ III first strand synthesis system for RT–PCR, *pfx* platinum DNA polymerase and NuPAGE Pre-cast gels were from Invitrogen. Tissue culture media and reagents were from Invitrogen. MyoD adenovirus (Ad5.f50.AdApt.Myod) was from Crucell (The Netherlands). Human embryonic kidney (HEK) 293 cells were obtained from ATCC. FuGENE 6 and complete protease inhibitors from Roche Applied Science (Indianapolis, IN, USA). Phospholipids were from Avanti Polar Lipids (Alabaster, AL, USA). All other chemicals were of analytical grade.

Methods

Patients. As *SEPN1* mutations have been identified in 50% of classical severe cases with multiple cores, PCR and direct

Table 2. Single-channel properties of WT and mutant RyR1s

Name	WT	Arg110Trp + Leu486Val	Asn2283His
In 250 mM KCl cis and trans			
K^+ conductance (pS)	801 ± 7 (17)	442 ± 77 (9)	786 ± 6 (10)
P_o at 2 μM Ca^{2+} cis at −35 mV	0.22 ± 0.04 (19)	0.70 ± 0.12 (7)	0.61 ± 0.07* (11)
P_o at 0.1 μM Ca^{2+} cis at −35 mV	0.0005 ± 0.0002 (4)	0.80 (2)	0.07 ± 0.04 (4)
In 250 mM KCl cis and trans + 10 mM Ca^{2+} trans			
$I_{Ca_{2+}}$ at 0 mV (pA)	−2.7 ± 0.1 (10)	0 (3)	−2.7 ± 0.1 (4)
P_o at 2 μM Ca^{2+} cis at 0 mV	0.03 ± 0.01 (3)	ND	0.35 ± 0.14 (4)
P_o at 0.1 μM Ca^{2+} cis at 0 mV	0.0003 ± 0.0001 (3)	ND	0.17 ± 0.14 (4)
E_{rev} (mV)	9.5 ± 0.2 (6)	ND	12.6 ± 0.2* (4)
P_{Ca}/P_K	7.0	ND	10.6

Data are the mean ± SE of number of experiments shown in parenthesis.
*$P < 0.05$ compared with WT RyR1.

sequencing of *SENP1* gene was performed in families 1 and 2 to exclude *SEPN1* mutations (data not shown).

Family 1. The compound heterozygous substitutions p.Ala 1577Thr + p.Gly2060Cys identified in the affected proband were inherited from the unaffected mother, who carried a G>A transition at position 4729 in exon 33 of the *RYR1*, resulting in the p.Ala1577Thr substitution, and from the una ffected father, who carried a G>T transition at position 6178 in exon 38 of the *RYR1*, resulting in the p.Gly2060Cys substitution. The carrier mother previously had one misca rriage. We obtained primary cultures of skeletal muscle cells from the proband and skin fibroblasts from the clinically una ffected parents, heterozygous for each substitution.

Family 2. The compound heterozygous substitutions p.Arg109 Trp + p.Met485Val resulting from a C>T transition at position 325 in exon 4 of the *RYR1* and from an A>G transition at position 1453 in exon 14 of the *RYR1* were identified in the homozygous state in the muscle cDNA of the two affected children, but in the heterozygous state in their genomic DNA. Their healthy father carried the compound heterozygous substitutions at the genomic level; the entire *RYR1* cDNA from the skeletal muscle of the healthy mother was sequenced and found to carry no substitutions, even in the promoter region. A muscle MRI showed a pattern of selective involvement similar to that observed in patients with CCD secondary to C-terminal *RYR1* mutations (13); however, the degree of muscle wasting was more pronounced, corresponding to a more severe clinical phenotype. Skin fibroblasts were obtained from the affected children and healthy parents.

Family 3. The compound heterozygous substitutions p.Ser71 Tyr + p.Asn2283His resulting from a C>A transition at position 212 in exon 3 of the *RYR1* and from an A>C transition at position 6847 in exon 42 of the *RYR1* were identified in the affected proband. The father carried the heterozygous substitution p.Ser71Tyr and the mother carried the heterozygous substitution p.Asn2283His. The patient was the first child of healthy unrelated parents. The family later had two healthy monozygotic twins (Fig. AF1–3). Skin fibroblasts were obtained from the proband but neither muscle tissue nor fibroblasts were available from the unaffected healthy parents.

Histological studies. Needle muscle biopsies were taken from the vastus lateralis under local anaesthesia after informed consent and processed for histological, histochemical and ultrastructural studies according to standard procedures (41).

Skeletal muscle cell lines and myoD-transduced fibroblasts. Human skeletal muscle cell cultures were established from a portion of the needle biopsy as previously described (24). Differentiation of myoblasts into myotubes was achieved by changing the medium from standard growth medium to differentiation medium [Dulbecco's modified Eagle' medium (DMEM) plus 4.5 mg/ml glucose, 0.5% BSA, 10 ng/ml EGF, 0.15 mg/ml creatine, 5 ng/ml insulin, 200 mM glutamine, 600 ng/ml penicillin G and streptomycin and 7 mM HEPES, pH 7.4).

For families 2 and 3, it was not possible to obtain myotubes from the muscle biopsies but primary skin fibroblast cultures were established from the probands and unaffected parents. Functional studies were performed on fibroblasts transduced with MyoD-encoding adenovirus in order to achieve myogenic conversion. Briefly, cells were plated on cover slips in 35 mM tissue culture dishes at a density of $\sim 1 \times 10^6$ cells/plate and allowed to grow at 37°C, 5% CO_2 in growth medium (DMEM supplemented with 10% fetal bovine serum). After allowing the cells to grow for 24 h, the adherent fibroblasts were infected by the addition of 1.6×10^8 virus particles (vp)/plate in differentiation medium (DMEM supplemented with 2% horse serum). After incubation for 3 h, cells were allowed to differentiate into multinucleated myotubes by culturing in DMEM plus 4.5 mg/ml glucose, 0.5% BSA, 10 ng/ml EGF, 0.15 mg/ml creatine, 5 ng/ml insulin, 200 mM glutamine, 600 ng/ml penicillin G and streptomycin, and 7 mM HEPES, pH 7.4 for 4–7 days. Such cells express desmin and other myofibrillar proteins and fuse into multinucleated myotubes under appropriate culture conditions (42).

Mutation screening. Total RNA was extracted from frozen skeletal muscle biopsies using the RNAeasy mini kit following manufacturer's instructions. Five micrograms of total RNA were used for each reverse transcription reaction; complementary DNA (cDNA) was synthesized using the SuperScript III first-strand synthesis system kit, in a final volume of 20 μl. The cDNAs were subsequently used for the following

amplification reactions: 27 overlapping fragments ranging from 400 to 1000 bp, covering the entire 15 kb coding sequence of the *RYR1* gene were amplified (primer sequences available on request). The reaction consisted of 0.5–1 μl cDNA as template, with 0.3 mM dNTPs, 1 mM $MgSO_4$, 0.3 μM of each primer, 1 U platinum *pfx* DNA polymerase, 1 *pfx* amplification buffer, 1 PCRx enhancer (for some GC-rich regions increased to three) in a total volume of 25 μl. PCR conditions were: denaturation at 95°C for 5 min followed by 30 cycles of 95°C for 15 s, annealing at primer-specific annealing temperatures (55–60°C) for 30 s, extension at 68°C for 30–90 s and a final extension step of 68°C for 10 min. Exon-specific primers (exons 3, 4, 14, 33, 38 and 42) were used when genomic DNA was amplified by PCR. All PCR products were purified and directly sequenced in both the forward and reverse directions using an ABI 3730XL by the MRC Genomics Core Laboratory.

Indirect immunofluorescence. Cells were fixed with an ice-cold solution of acetone: methanol (1:1) and then labelled with the following primary antibodies: mouse anti-MyoD monoclonal antibody (1:200 dilution), mouse anti-desmin monoclonal antibody (1:50 dilution), mouse anti-slow muscle myosin monoclonal antibody (1:20 dilution), goat anti-DHPR polyclonal antibody (1:1000 dilution) and mouse anti-RyR1 monoclonal antibody (1:1000 dilution in PBS). Cover slips were washed three times and then incubated with anti-mouse or anti-goat biotinylated secondary antibody (1:200 dilution) for 30 min. After three further washes, cells were incubated at room temperature for 20 min with streptavidin-conjugated Alexa-594 (1:1000 dilution). Cells were washed three times and nuclei were stained with Hoechst 33258 for 10 min. Cover slips were mounted in aqueous mounting medium and viewed with a fluorescent Leica DMR fluorescent microscope (Leica, Germany) linked to a Prior filter wheel, equipped with 20×/0.5 HC PL FLUOTAR objective; images were digitally captured using Metamorph software (Universal Imaging Inc.). All washes and dilutions were in phosphate-buffered saline.

Intracellular calcium measurements. Changes in the intracellular Ca^{2+} concentration, $[Ca^{2+}]_i$, of the myotubes were monitored with the fluorescent Ca^{2+} indicator fura-2 at the single cell level by digital imaging microscopy as previously described (26). Individual cells were stimulated with a 12-way 100 mM diameter quartz micromanifold computer controlled microperfuser (ALA Scientific) as described. On-line (340, 380 nm and ratio) measurements were recorded using a fluorescent Axiovert S100 TV inverted microscope (Carl Zeiss GmbH, Jena, Germany) equipped with a 20× water-immersion FLUAR objective (0.17 NA), filters (BP 340/380, FT 425, BP 500/530). The cells were analysed using an Openlab imaging system and the average pixel value for each cell was measured at excitation wavelengths of 340 and 380 nm.

Changes in the $[Ca^{2+}]_i$ in response to caffeine and 4-chloro-*m*-cresol in HEK293 cells expressing WT and mutant rabbit cDNA RyR1s was monitored with the fluorescent Ca^{2+} indicator Fluo-4. Briefly, HEK293 cells grown on glass cover slips were washed three times with PBS buffer and loaded with 5 μM Fluo 4-AM for 1 h at 37°C in Krebs–Ringer–Henseleit (KRH) buffer (125 mM NaCl, 5 mM KCl, 1.2 mM KH_2PO_4, 6 mM glucose, 1.2 mM $MgCl_2$, 2 mM $CaCl_2$ and 25 mM HEPES, pH 7.4). After loading, cells were rinsed with KRH buffer to remove non-hydrolysed fluophore and kept in KRH buffer for 30 min to complete de-esterification. Individual cells in KRH buffer were defined as region of interest, and average fluorescence increase in response to addition of 10 mM caffeine or 400 μM 4-chloro-*m*-cresol was measured, using the program ImageMaster (Photon Technology International, Lawrenceville, NJ, USA).

Construction of mutant cDNAs. Single and multiple base changes of rabbit RyR1 cDNA were performed by *Pfu*-turbo polymerase-based chain reaction using mutagenic oligonucleotides and the QuikChange site-directed mutagenesis kit (Stratagene, La Jolla, CA, USA) as described previously (43). Briefly, subfragments of RyR1 cDNA, subcloned into cloning vectors, served as a template for PCR. The *Cla*I/*Aau*I (polylinker-1361) fragment was used for Ser71Tyr and Arg110Trp mutations (corresponding to the human residues Ser71Tyr and Arg109Trp, the *Aau*I/*Not*I (1361–2514) for Leu486Val (corresponding to the human residues Met485Val), the *Aat*II/*Pin*AI (3470–5066) for Ala1578Thr (corresponding to the human residues Ala1577Thr) the *Pin*AI/*Xho*I (5066–6598) for Ser2060Cys (corresponding to the human residues Gly2060Cys) and the *Xho*I–*Bbr*PI (6598–7692) for Asn2283His. The complete mutated fragments amplified by PCR were confirmed by DNA sequencing. The fragments with mutations were cloned back into the original positions by standard cloning techniques. Finally, expression plasmids for full-length RyR1 with the mutations were constructed by ligating three RyR1 fragments [*Cla*I/*Xho*I (polylinker-6598), *Xho*I/*Eco*RI (6598–11767), *EcoRI*/*XbaI* (11767-polylinker)] and pCMV5 (*Cla*I/*Xba*I) expression vector. Nucleotide numbering is as described previously (44).

Expression of WT and mutant ryr1 proteins in hek293 cells. WT RyR1 and mutant cDNAs were transiently expressed in HEK293 cells transfected with FuGENE 6 according to manufacturer's instructions. Cells were maintained at 37°C and 5% CO_2 in high glucose DMEM containing 10% fetal bovine serum and plated the day before transfection. For each 10 cm tissue culture dish, 3.5 μg of cDNA was used. Cells were harvested 48 h after transfection. Crude membrane fractions and proteolipoosmes containing the purified RyR1s were prepared in the presence of protease inhibitors as described (43).

Immunoblot analyses. Skeletal muscle proteins were extracted in sample buffer consisting of 75 mM Tris–HCl, 1% SDS, plus a cocktail of protease inhibitors (antipain, aprotinin and leupeptin). Thirty microgram of proteins were resolved using a NuPAGE Pre-cast gels (3–8% Tris-acetate, Invitrogen) and then transferred electrophoretically to nitrocellulose membrane. Nitrocellulose membrane was blocked in 10% semi skimmed milk in Tris-buffered saline buffer and then probed with mouse anti-RyR1 monoclonal antibody and mouse anti-desmin monoclonal antibody at room temperature for 1 h.

After washing, membranes were incubated with HRP-anti-mouse IgG for 1 h at room temperature. Immunoreactivity was visualized using chemiluminescence.

Twenty micrograms protein of crude membrane fractions prepared from HEK293 cells were separated by 3–12% SDS/PAGE, transferred to polyvinylidene difluoride membranes and probed with antibody specific for RyR1 as described (44). Western blots were developed using 3,3-diaminobenzidine and H_2O_2 and quantified using Kodak Digital Science ID.

[^{3}H]Ryanodine binding. [^{3}H]Ryanodine binding experiments were performed with crude membrane fractions prepared from HEK 293 cells. Unless otherwise indicated, membranes were incubated with 3 nM [^{3}H]ryanodine in 20 mM imidazole, pH 7.0, 0.15 M sucrose, 250 mM KCl, 1 mM glutathione (oxidized), protease inhibitors and indicated Ca^{2+} and caffeine concentrations. Non-specific binding was determined using a 1000–2000-fold excess of unlabelled ryanodine. After 20 h, samples were diluted with eight volumes of ice-cold water and placed on Whatman GF/B filters pre-incubated with 2% polyethyleneimine in water. Filters were washed three times with 5 ml ice-cold 100 mM KCl, 1 mM KPipes, pH 7.0 solution. The radioactivity remaining bound to the filters was determined by liquid scintillation counting to obtain bound [^{3}H]ryanodine.

B_{max} values of [^{3}H]ryanodine binding were determined by incubating membranes for 4 h at 24°C with a saturating concentration of [^{3}H]ryanodine (30 nM) in 20 mM imidazole, pH 7.0, 0.6 M KCl, 0.15 M sucrose, 1 mM glutathione (oxidized), protease inhibitors and 100 μM Ca^{2+}. Specific binding was determined as described above.

Single-channel recordings. Single-channel measurements were performed using planar lipid bilayers containing a 5:3:2 mixture of bovine brain phosphatidylethanolamine, phosphatidylserine and phosphatidylcholine (25 mg of total phospholipid/ml *n*-decane as previously described (45). Proteoliposomes containing the purified recombinant RyR1s were added to the *cis* (SR cytosolic side) chamber of a bilayer apparatus and fused in the presence of an osmotic gradient (250 mM cis KCl/20 mM trans KCl in 20 mM KHEPES, pH 7.4, 2 mM Ca^{2+}). After the appearance of channel activity, trans (SR lumenal side) KCl concentration was increased to 250 mM to prevent further fusion of proteoliposomes. To determine K^+ and Ca^{2+} conductances and permeability ratios, single-channel activities were recorded in symLeurical 250 mM KCl solution before and after addition of 10 mM Ca^{2+} to the trans side and analysed as described (45).

Statistical analysis. Statistical analysis was performed using the Student's *t*-test for paired samples or using ANOVA when more than two groups were compared. Origin computer program (Microcal Software, Inc., Northampton, MA, USA) was used for statistical analysis and dose–response curve generation. The EC_{50} and R_{max} values were calculated using the Origin program from sigmoidal curve fitting of all the data points.

ACKNOWLEDGEMENTS

This work was supported by the Department of Anesthesia Basel University Hospital, grant 3200-067820.02 of the SNF (to S.T.), grant RA2/670/2 supported by Muscular Dystrophy Campaign of Great Britain and North Ireland (to F.M.), NIH AR 18687 (to G.M.) and by grants from the Swiss Muscle Foundation and Association Française Contre les Myopathies.

Conflict of Interest statement. None declared.

REFERENCES

1. Fleischer, S. and Inui, M. (1989) Biochemistry and biophysics of excitation–contraction coupling. *Annu. Rev. Biophys. Biophys. Chem.*, **18**, 333–364.
2. Franzini-Armstrong, C. and Jorgensen, A.O. (1994) Structure and development of E–C coupling units in skeletal muscle. *Annu. Rev. Physiol.*, **56**, 509–534.
3. Lamb, G.D. and Stephenson, D.G. (1990) Control of calcium release and the effect of ryanodine in skinned muscle fibres of the toad. *J. Physiol. (Lond.)*, **423**, 519–542.
4. Meissner, G. (1994) Ryanodine receptor/Ca^{2+} release channels and their regulation by endogenous effectors. *Annu. Rev. Physiol.*, **56**, 485–508.
5. Phillips, M.S., Fujii, J., Khanna, V.K., DeLeon, S., Yokobata, K., de Jong, P.J. and MacLennan, D.H. (1996) The structural organization of the human skeletal muscle ryanodine receptor (*RYR1*) gene. *Genomics*, **34**, 24–41.
6. Rios, E. and Pizarro, G. (1991) Voltage sensor of excitation–contraction coupling in skeletal muscle. *Physiol. Rev.*, **71**, 849–908.
7. McCarthy, T.V., Quane, K.A. and Lynch, P.J. (2000) Ryanodine receptor mutations in malignant hyperthermia and central core disease. *Hum. Mutat.*, **15**, 410–417.
8. Jurkat-Rott, K., McCarthy, T. and Lehmann-Horn, F. (2000) Genetics and pathogenesis of malignant hyperthermia. *Muscle Nerve*, **23**, 4–17.
9. Lyfenko, A.D., Goonasekera, S.A. and Dirksen, R.T. (2004) Dynamic alterations in myoplasmic Ca^{2+} in malignant hyperthermia and central core disease. *Biochem. Biophys. Res. Commun.*, **322**, 1256–1266.
10. Treves, S., Anderson, A.A., Ducreux, S., Divet, A., Bleunven, C., Grasso, C., Paesante, S. and Zorzato, F. (2005) Ryanodine receptor 1 mutations, dysregulation of calcium homeostasis and neuromuscular disorders. *Neuromuscul. Disord.*, **15**, 577–587.
11. Ferreiro, A., Monnier, N., Romero, N.B., Leroy, J.P., Bönnemann, C., Haenggeli, C.A., Straub, V., Voss, W.D., Nivoche, Y., Jungbluth, H. *et al*. (2002) A recessive form of central core disease, transiently presenting as multi-minicore disease, is associated with a homozygous mutation in the ryanodine receptor type 1 gene. *Ann. Neurol*, **51**, 750–759.
12. Jungbluth, H., Müller, C.R., Halliger-Keller, B., Brockington, M., Brown, S.C., Feng, L., Chattopadhyay, A., Mercuri, E., Manzur, A.Y., Ferreiro, A. *et al*. (2002) Autosomal recessive inheritance of RYR1 mutations in a congenital myopathy with cores. *Neurology*, **59**, 284–287.
13. Jungbluth, H., Davis, M.R., Muller, C., Counsell, S., Allsop, J., Chattopadhyay, A., Messina, S., Mercuri, E., Laing, N.G., Sewry, C.A., Bydder, G. and Muntoni, F. (2004) Magnetic resonance imaging of muscle in congenital myopathies associated with RYR1 mutations. *Neuromuscul. Disord.*, **14**, 785–790.
14. Guis, S., Figarella-Branger, D., Monnier, N., Bendahan, D., Kozak-Ribbens, G., Mattei, J.P., Lunardi, J., Cozzone, P.J. and Pellissier, J.F. (2004) Multiminicore disease in a family susceptible to malignant hyperthermia: histology, *in vitro* contracture tests, and genetic characterization. *Arch. Neurol.*, **61**, 106–113.
15. Romero, N.B., Monnier, N., Viollet, L., Cortey, A., Chevallay, M., Leroy, J.P., Lunardi, J. and Fardeau, M. (2003) Dominant and recessive central core disease associated with RYR1 mutations and fetal akinesia. *Brain*, **126**, 2341–2349.
16. Zhang, Y., Chen, H.S., Khanna, V.K., De Leon, S., Phillips, M.S., Schappert, K., Britt, B.A., Browell, A.K. and MacLennan, D.H. (1993) A mutation in the human ryanodine receptor gene associated with central core disease. *Nat. Genet.*, **5**, 46–50.

17. Davis, M.R., Haan, E., Jungbluth, H., Sewry, C., North, K., Muntoni, F., Kuntzer, T., Lamont, F., Bankier, A., Tomlinson, P. *et al*. (2003) Principal mutation hotspot for central core disease and related myopathies in the C-terminal transmembrane region of the *RYR1* gene. *Neuromuscul. Disord.*, **13**, 151–157.
18. Monnier, N., Romero, N.B., Lerale, J., Nivoche, Y., Qi, D., MacLennan, D.H., Fardeau, M. and Lunardi, J. (2000) An autosomal dominant congenital myopathy with cores and rods is associated with a neomutation in the RYR1 gene encoding the skeletal muscle ryanodine receptor. *Hum. Mol. Genet.*, **9**, 2599–2608.
19. Monnier, N., Romero, N.B., Lerale, J., Landrieu, P., Nivoche, Y., Fardeau, M. and Lunardi, J. (2001) Familial and sporadic forms of central core disease are associated with mutations in the C-terminal domain of the skeletal muscle ryanodine receptor. *Hum. Mol. Genet.*, **10**, 2581–2592.
20. Tilgen, N., Zorzato, F., Halliger-Keller, B., Muntoni, F., Sewry, C., Palmucci, L.M., Schneider, C., Hauser, E., Lehmann-Horn, F., Müller, C.R. and Treves, S. (2001) Identification of four novel mutations in the C-terminal membrane spanning domain of the ryanodine receptor 1: association with central core disease and alteration of calcium homeostasis. *Hum. Mol. Genet.*, **10**, 2879–2887.
21. Zorzato, F., Yamaguchi, N., Xu, L., Meissner, G., Müller, C.R., Pouliquin, P., Muntoni, F., Sewry, C., Girard, T. and Treves, S. (2003) Clinical and functional effects of a deletion in a COOH-terminal lumenal loop of the skeletal muscle ryanodine receptor. *Hum. Mol. Genet.*, **12**, 379–388.
22. Treves, S., Larini, F., Menegazzi, P., Steinberg, T.H., Koval, M., Vilsen, B., Andersen, J.P. and Zorzato, F. (1994) Alteration of intracellular Ca2+ transients in COS-7 cells transfected with the cDNA encoding skeletal-muscle ryanodine receptor carrying a mutation associated with malignant hyperthermia. *Biochem. J.*, **301**, 661–665.
23. Otsu, K., Nishida, K., Kimura, Y., Kuzuya, T., Hori, M., Kamada, T. and Tada, M. (1994) The point mutation Arg615→Cys in the Ca2+ release channel of skeletal sarcoplasmic reticulum is responsible for hypersensitivity to caffeine and halothane in malignant hyperthermia. *J. Biol. Chem.*, **269**, 9413–9415.
24. Censier, K., Urwyler, A., Zorzato, F. and Treves, S. (1998) Intracellular calcium homeostasis in human primary muscle cells from malignant hyperthermia-susceptible and normal individuals. Effect Of overexpression of recombinant wild-type and Arg163Cys mutated ryanodine receptors. *J. Clin. Invest.*, **101**, 1233–1242.
25. Owen, V.J., Taske, N.L. and Lamb, G.D. (1997) Reduced Mg2+ inhibition of Ca2+ release in muscle fibers of pigs susceptible to malignant hyperthermia. *Am. J. Physiol. Cell Physiol.*, **272**, C203–C211.
26. Ducreux, S., Zorzato, F., Müller, C.R., Sewry, C., Muntoni, F., Quinlivan, R., Restagno, G., Girard, T. and Treves, S. (2004) Effect of ryanodine receptor mutations on IL-6 release and intracellular calcium homeostasis in human myotubes from malignant hyperthermia susceptible individuals and patients affected by central core disease. *J. Biol. Chem.*, **279**, 43838–43846.
27. Avila, G., O'Brien, J.J. and Dirksen, R.T. (2001) Excitation–contraction uncoupling by a human central core disease mutation in the ryanodine receptor. *Proc. Natl Acad. Sci. USA*, **98**, 4215–4220.
28. Avila, G., O'Connell, K.M. and Dirksen, R.T. (2003) The pore region of the skeletal muscle ryanodine receptor is a primary locus for excitation–contraction uncoupling in central core disease. *J. Gen. Physiol.*, **121**, 277–286.
29. Lynch, P.J., Krivosic-Horber, R., Reyford, H., Monnier, N., Quane, K., Adnet, P., Haudecoeur, G., Krivosic, I., McCarthy, T. and Lunardi, J. (1997) Identification of heterozygous and homozygous individuals with the novel RYR1 mutation Cys35Arg in a large kindred. *Anesthesiology*, **86**, 620–626.
30. Ducreux, S., Zorzato, F., Ferreiro, A., Jungbluth, H., Muntoni, F., Monnier, N., Müller, C.R. and Treves, S. (2006) Functional properties of ryanodine receptors carrying 3 amino acid substitutions identified in patients affected by multi-minicore disease and central core disease, expressed in immortalised lymphocytes. *Biochem. J.*, **395**, 259–266.
31. Gillard, E.F., Otsu, K., Fujii, J., Duff, C., de Leon, S., Khanna, V.K., Britt, B.A., Worton, R.G. and MacLennan, D.H. (1992) Polymorphisms and deduced amino acid substitutions in the coding sequence of the ryanodine receptor (*RYR1*) gene in individuals with malignant hyperthermia. *Genomics*, **13**, 1247–1254.
32. Sutko, J.L., Airey, J.A., Welch, W. and Ruest, L. (1997) The pharmacology of ryanodine and related compounds. *Pharmacol. Rev*, **49**, 53–98.
33. Jungbluth, H., Sewry, C., Brown, S.C., Manzur, A.Y., Mercuri, E., Bushby, K., Rowe, P., Johnson, M.A., Hughes, I., Kelsey, A., Dubowitz, V. and Muntoni, F. (2000) Minicore myopathy in children—a clinical and histopathological study of 19 cases. *Neuromuscul. Disord.*, **10**, 264–273.
34. Ferreiro, A., Estournet, B., Chateau, D., Romero, N.B., Laroche, C., Odent, S., Toutain, A., Cabello, A., Fontan, D., dos Santos, H.G. *et al*. (2000) Multi-minicore disease—searching for boundaries: phenotype analysis of 38 cases. *Ann. Neurol.*, **48**, 745–757.
35. Monnier, N., Ferreiro, A., Marty, I., Labarre-Vila, A., Mezin, P. and Lunardi, J. (2003) A homozygous splicing mutation causing depletion of skeletal muscle RYR1 is associated with multi-minicore disease congenital myopathy with ophthalmoplegia. *Hum. Mol. Genet.*, **12**, 1171–1178.
36. Lopez, J.R., Linares, N., Pessah, I.N. and Allen, P.D. (2005) Enhanced response to caffeine and 4-chloro-*m*-cresol in malignant hyperthermia-susceptible muscle is related in part to chronically elevated resting [Ca2+]*i*. *Am. J. Physiol. Cell Physiol.*, **288**, C606–C612.
37. Fessenden, J.D., Wang, Y., Moore, R.A., Chen, S.R., Allen, P.D. and Pessah, I.N. (2000) Divergent functional properties of ryanodine receptor type 1 and 3 expressed in a myogenic cell line. *Biophys. J.*, **79**, 2509–2525.
38. Matyash, M., Matyash, V., Nolte, C., Sorrentino, V. and Kettenmann, H. (2001) Requirement of functional ryanodine receptor type 3 for astrocyte migration. *FASEB J.*, **16**, 84–96.
39. Konig, S., Hinard, V., Arnaudeau, S., Holzer, N., Potter, G., Bader, C.R. and Bernheim, L. (2004) Membrane hyperpolarization triggers myogenin and myocyte enhancer factor-2 expression during human myoblast differentiation. *J. Biol. Chem.*, **279**, 28287–28296.
40. Bijlenga, P., Liu, J.H., Espinos, E., Haenggeli, C.A., Fischer-Lougheed, J., Bader, C.R. and Bernheim, L. (2000) T-type a1H Ca2+ channels are involved in Ca2+ signaling during terminal differentiation (fusion) of human myoblasts. *Proc. Natl Acad. Sci. USA*, **97**, 7627–7632.
41. Jungbluth, H., Sewry, C., Brown, S.C., Manzur, A.Y., Mercuri, E., Bushby, K., Rowe, P., Johnson, M.A., Hughes, I., Kelsey, A., Dubowitz, V. and Muntoni, F. (2002) Minicore myopathy in children: a clinical and histopathological study of 19 cases. *Neuromuscul. Disord.*, **10**, 264–273.
42. Lattanzi, L., Salvatori, G., Coletta, M., Sonnino, C., Cusella De Angelis, M.G., Gioglio, L., Murry, C.E., Kelly, R., Ferrari, G., Molinaro, M. *et al*. (1998) High efficiency myogenic conversion of human fibroblasts by adenoviral vector-mediated MyoD gene transfer. An alternative strategy for *ex vivo* gene therapy of primary myopathies. *J. Clin. Invest.*, **101**, 2119–2128.
43. Gao, L., Balshaw, D., Xu, L., Tripathy, A., Xin, C. and Meissner, G. (2000) Evidence for a role of the lumenal M3–M4 loop in skeletal muscle Ca(2+) release channel (ryanodine receptor) activity and conductance. *Biophys. J.*, **79**, 828–840.
44. Takeshima, H. (1993) Primary structure and expression from cDNAs of the ryanodine receptor. *Ann. NY Acad. Sci.*, **707**, 165–177.
45. Xu, L., Wang, Y., Gillespie, D. and Meissner, G. (2006) Two rings of negative charges in the cytosolic vestibule of type-1 ryanodine receptor modulate ion fluxes. *Biophys. J.*, **90**, 443–453.